NEURAL SYNCHRONIZATION LANDSCAPES REVEAL ALTERED STRUCTURE–FUNCTION COUPLING IN NEURODEGENERATIVE DISEASES

Anonymous authors
Paper under double-blind review

ABSTRACT

Modern neuroimaging technologies enable the study of structural connectivity (SC) and functional connectivity (FC) *in vivo*. However, due to the distinct biological underpinnings of SC and FC, understanding how the altered coupling mechanism is associated with the progression of neurodegeneration remains a challenge in the neuroscience field. Drawing inspiration from the rich neural dynamics captured by the Kuramoto model, we introduce a brain-inspired neural network, coined *KM-Net*, to explain cognitive behavior from neuroimages, which is rooted in the neuroscience principle of oscillatory synchronization. Given that disrupted synchronization in neural oscillations closely underlines neurodegenerative diseases, we further extend *KM-Net* to an explainable deep model in the arena of disease early diagnosis. By capturing the emergence of synchronized FC patterns from the underlying SC architecture, our approach provides a biologically informed representation for the dynamical system of functional fluctuations. We validate our novel computational framework through extensive experiments on a diverse set of neuroimaging cohorts, demonstrating its effectiveness in characterizing cognition-relevant brain fingerprint and disease-specific imaging biomarkers. Together, promising results indicate the potential of neural synchronization modeling for advancing computational neuroscience and improving the understanding of neurodegenerative diseases.

1 INTRODUCTION

Neurodegenerative diseases (ND), including Alzheimer's disease (AD) (Scheltens et al., 2021), Parkinson's disease (PD) (Bloem et al., 2021) and frontotemporal dementia (FTD), represent an escalating global health crisis. Together they already affect more than 50 million people worldwide, a number expected to exceed 130 million by 2050 as populations age (Prince et al., 2015; Ehrenberg et al., 2020). The human cost is mirrored by an economic burden that has surpassed US$1 trillion annually (Jeromin & Bowser, 2017). Despite decades of research, no disease-modifying therapies exist (Cummings, 2017); clinical care remains largely symptomatic (Lang, 2010) and is typically initiated only after irreversible neuronal loss.

A growing body of evidence shows that pathogenic cascades begin years—often decades—before overt clinical presentation. In AD, amyloid-β (Aβ) aggregates can be detected up to 30 years prior to symptom onset, seeding tauopathy and progressive neurodegeneration (Donohue et al., 2017). In PD, nonmotor prodromes such as hyposmia and REM (rapid eye movement) sleep behavior disorder emerge 5-10 years before motor signs, reflecting early disruption of extranigral circuits (Jansen et al., 2015; Wolk et al., 2018). FTD likewise shows subtle behavioural and network-level changes prior to the onset of clinical symptoms. These prolonged presymptomatic phases offer a critical therapeutic window, given that disease can be detected early and with sufficient specificity. Although biomarkers like PET imaging and CSF assays have achieved remarkable success, their high cost and limited accessibility have hindered their use in routine disease screening. In this regard, there is a strong need for early detection of neurodegenerative diseases using widely available techniques such as MRI (Magnetic Resonance Imaging).

Structural–functional coupling is an early marker for NDs. The brain's wiring mechanism offers a complementary, systems-level vantage point on disease progression. Of particular interest is the coupling between structural connectivity (SC) and functional connectivity (FC)—the degree to which the brain's anatomical scaffold constrains its dynamic activity. Mounting evidence shows that SC–FC coupling is disrupted as neurodegeneration starts in NCs (Zou et al., 2024). For example, (Sun et al., 2024) observed altered SC-FC coupling patterns in parietal, occipitotemporal, motor, and association cortices, which is associated with widespread motor and non-motor symptomatology in AD. Convergent findings from behavioural and language variants of FTD further implicate early breakdown in transmodal networks, with social-cognitive deficits and executive dysfunction observed in bvFTD and PPA subtypes (Harciarek & Cosentino, 2013). Across NDs, SC–FC alteration emerges as a reproducible signature of brain network disruption, which precedes forthcoming structure atrophy through the lens of impaired neuro-synchronization. Because SC-FC coupling is anchored in brain anatomy yet sensitive to functional fluctuations, an in-depth understanding of the coupling mechanism might provide an interpretable biomarker that generalizes across disease boundaries.

From concept to measurable biomarker. Building on this rationale, we propose to elevate *neural oscillatory synchronization*, aka. the magnitude of brain-wide phase coordination, into a quantifiable, clinically actionable biomarker. To achieve it, we introduce *KM-Net*, a biologically grounded deep model, principled in Kuramoto model (Kuramoto, 1975), that characterizes phase-coupled dynamics of functional fluctuations from coupled brain regions wired by neural fibers. By uncovering how disease-specific alterations disrupt large-scale neural synchrony in the brain, our *KM-Net* is designed to not only predict the dementia risk for individual old adults but also identify focal patterns associated with the altered SC-FC coupling mechanism in NDs.

Our work. Our contributions to this work are three-fold:

- We cast neurodegeneration as a systems-level disruption of SC-constrained neural synchronization and formalise its quantification with a brain-inspired deep model rooted in the dynamics of the Kuramoto model (as shown in Fig. 1).
- We have uncovered anatomically interpretable synchronization patterns using machine learning techniques that generalize multiple neurodegenerative disorders in the framework of SC-FC coupling.
- We present *state-of-the-art* early diagnostic approaches for AD, PD, and FTD, with great potential to be deployed in routine clinical practice.

By reframing neurodegeneration as a system-level disruption of brain-wide phase coordination rather than isolated regional deficits, our framework offers a scalable and interpretable data-driven approach toward earlier detection and data-driven therapeutic targeting.

2 Related Works

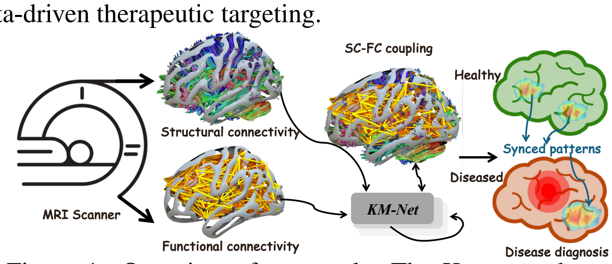

Figure 1: Overview of our work. The Kuramoto-based model (*KM-Net*) captures network-wide synchronization dynamics and links SC–FC coupling to neurodegeneration progression.

The human brain is perhaps the most complex system in the universe, with its regions interconnected by neuronal fibers that support self-organized functional fluctuations underlying diverse cognitive processes and behaviors. Many neurodegenerative diseases might hijack the communication system to spread neuropathology throughout the brain. In light of this, it is critical to understand the coupling mechanism between SC and FC, which could potentially serve as a putative biomarker for the early diagnosis across NDs. In this section, we briefly review previous works on computational approaches to SC-FC coupling and Kuramoto-based modeling for whole-brain functional fluctuations.

Computational approaches to SC–FC coupling. Early work assessed structure–function coupling with simple correlations between regional SC profiles and resting-state FC, or with generative communication models that simulate how information might flow over the structural scaffold (e.g., shortest-path (Goñi et al., 2014), communicability (Honey et al., 2009), and diffusion metrics (Abdelnour et al., 2014)). Recent large-scale studies have refined these ideas by (i) treating SC-FC coupling as a region-specific rather than global property and (ii) exploring how coupling changes with behavioural demands. For example, (Popp et al., 2025) showed that task-dependent variations in SC–FC coupling predict individual intelligence scores across $>$700 Human Connectome Project participants, emphasising that coupling is dynamic and context-sensitive.

SC-FC coupling has also been proven as a putative biomarker of neurodegeneration. A multicentre AD study by (Sun et al., 2024) reported early SC-FC alterations in transmodal cortex that are associated with CSF-tau and cognitive decline independently of atrophy. Machine-learning pipelines that combine static and time-resolved (dynamic) coupling further boost diagnostic accuracy: (Wu et al., 2025) achieved AUCs $\approx$0.9 for distinguishing healthy controls (HC), individuals with mild cognitive impairment (MCI), and AD by using static + dynamic coupling features into a Gaussian-naive-Bayes classifier. Significant alterations of SC-FC coupling have now been documented in Parkinson's disease and frontotemporal dementia, but existing work typically analyses each ND separately and relies on hand-crafted SC-FC coupling measures, which are less reproducible across neuroimaging studies.

Kuramoto-based whole-brain modeling. The Kuramoto-based phase oscillator framework offers a mechanistic route to link SC to emergent FC. Early applications used empirical SC as the coupling matrix and tuned a global coupling constant to reproduce resting-state fMRI correlations (Honey et al., 2009; Cabral et al., 2011). Current research extends this framework in two main directions.

Biophysical realism & multiscale structure – Hierarchical modeling approaches have recently gained traction for capturing the multi-scale nature of brain dynamics. Specifically, hierarchical extensions of neural oscillatory models embed fast, local modules within slower, large-scale oscillatory structures, enabling a more accurate representation of both spatial and temporal organization in brain activity. For example, the hierarchical Kuramoto model for the human cortex introduced by Myrov et al. (Myrov et al., 2024) leverages a two-tiered system of coupled oscillators to simultaneously capture local synchronization phenomena and long-range coordination across brain regions.

Disease and perturbation studies – Hopfield-Kuramoto hybrid models have been proposed to encode multiple wave-pattern attractors and replicate dominant fMRI modes (Yao et al., 2025), which has been used to predict lesion-induced changes in FC (Rayfield et al., 2025). However, most models fix coupling weights or tune only global parameters, limiting the applicability in disease diagnosis at an individual level.

Positioning of the present work. The literature therefore leaves two key gaps: (1) *Lack system-level understanding.* Existing correlation-based methods primarily target localized SC-FC disruptions but fall short of providing a system-level understanding of how SC-FC coupling contributes mechanistically to disease progression. (2) *Lack model explainability across NDs.* Although various deep models have been proposed, few are specifically designed to uncover novel biological mechanisms underlying NDs.

Our *KM-Net* framework bridges these gaps by understanding phase-coupled neural oscillatory synchronization and deriving novel imaging biomarker from the learned SC-FC coupling mechanism that (i) quantify mechanistic role of SC–FC alteration in NDs, (ii) generate putative biomarkers of SC-FC coupling across AD, PD, and FTD, and (iii) yield state-of-the-art performance for presymptomatic diagnosis while remaining clinically interpretable.

3 METHODS

3.1 PRELIMINARY

Brain network construction. *First*, we construct SC from diffusion-weighted imaging (DWI) using fiber tractography, where the SC matrix $S \in \mathbb{R}^{N\times N}$ represents the connection strength between N brain regions. Each element s_{ij} is defined as: $s_{ij} = \frac{c_{ij}}{\sum_{k\neq i} c_{ik}}$, where c_{ij} is the streamline count between regions i and j. *Second*, FC is computed from resting-state fMRI by measuring the Pearson's correlation between the blood oxygen level-dependent (BOLD) time series between different brain regions. The FC matrix $E \in \mathbb{R}^{N\times N}$ is given by: $E_{ij} = \frac{\mathrm{cov}(x_i, x_j)}{\sigma_{x_i}\sigma_{x_j}}$, where x_i and

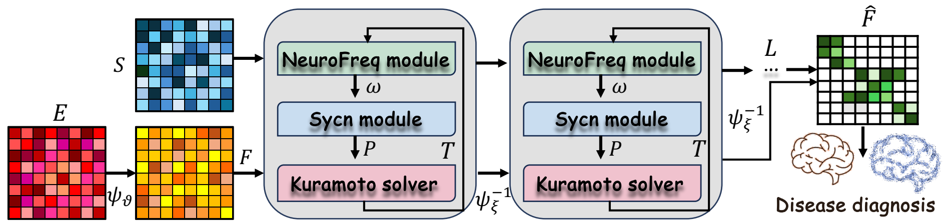

Figure 2: The network architecture of our proposed *KM-Net*.

x_j are the BOLD signals of regions i and j. They establish the foundation for analyzing SC-FC coupling in brain networks.

The Kuramoto model for oscillator synchronization. The Kuramoto model describes the emergence of synchronization in coupled phase oscillators, with applications across many fields. Each oscillator i evolves according to: $\frac{d\theta_i}{dt} = \omega_i + \frac{K}{N}\sum_{j=1}^{N}\sin(\theta_j - \theta_i)$, where θ_i represents the phase, ω_i the intrinsic frequency, and K the coupling strength (Rodrigues et al., 2016).

3.2 I: *KM-Net*: Scalable Kuramoto-Based Neural Synchronization

Our *KM-Net* extends the classic Kuramoto model to describe how FC emerges from SC through neural phase synchronization. Unlike traditional SC-FC coupling models that rely on statistical correlations or deep learning without clear mechanistic insights (Dan et al., 2023; Mazumder et al., 2024; Li et al., 2018), we propose a physics-based, brain-inspired, learnable framework. Our *KM-Net* integrates oscillator dynamics, adaptive synchronization, and hierarchical memory encoding, dynamically estimating frequencies, refining phase interactions, and stabilizing functional fluctuations. Specifically, *KM-Net* consists of three core modules: the *NeuroFreq module*, which learns intrinsic oscillation frequencies; the *Sync module*, which refines phase interactions using a bidirectional coupling mechanism; and the *Kuramoto solver*, which iteratively integrates past oscillatory states to stabilize functional emergence. The network architecture of *KM-Net* is shown in Fig. 2.

Intrinsic frequency estimation via NeuroFreq module. The *NeuroFreq module* learns the intrinsic frequencies of neural oscillators, avoiding fixed distributions and instead dynamically parameterizing oscillation rates through a structured anti-symmetric transformation. Each oscillator i evolves according to the modified scalable Kuramoto equation:

$$\frac{d\boldsymbol{f}_i}{dt} = \boldsymbol{\omega}_i + \lambda(\boldsymbol{s}_i + \sum\nolimits_{j=1}^{N} s_{ij}\boldsymbol{f}_i), \tag{1}$$

where $\boldsymbol{f}_i(t) \in \mathbb{R}^N$ represents the vector-based oscillator's phase information of region i (we omit the index t for simplicity), derived from the FC through a mapping function $F = \psi_\vartheta(E)$. ψ_ϑ encodes FC into an oscillatory representation, modeling each brain region as a dynamic oscillator. s_{ij} is the SC matrix defining coupling strengths at region (i, j), λ is the global coupling coefficient. Unlike traditional methods that assume $\boldsymbol{\omega}_i$ follows a predefined Gaussian distribution, we introduce a learnable transformation matrix Ω to parameterize intrinsic frequencies adaptively:

$$\boldsymbol{\omega}_i = \Omega_i\boldsymbol{f}_i, \quad \text{where} \quad \Omega = -\Omega^\intercal, \tag{2}$$

where Ω is constrained to be anti-symmetric to enforce realistic frequency shifts. This learned frequency dynamically modulates the oscillator phase evolution, leading to subject-specific synchronization behavior. The transformation ensures that oscillatory trajectories remain aligned with empirical neuroimaging observations rather than being stereotyped by arbitrary statistical priors. To maintain numerical stability, the transformed oscillations are expanded to align with the batch and time dimensions: $\boldsymbol{\omega}_{b,t,i} = |\Omega_i\boldsymbol{f}_i|, \quad \forall b \in [1, B], \quad t \in [1, T], \quad i \in [1, N]$, where B, T represent the batch and time dimensions, and the expansion aligns the frequency tensor with temporal oscillatory updates.

Neural synchronization via Sync module. The *Sync module* refines phase interactions between brain regions by incorporating SC as a constraint while dynamically adapting interaction strengths through a learned synchronization matrix. Unlike classical Kuramoto models, which assume a fixed adjacency matrix S, we introduce a trainable coupling matrix $P \in \mathbb{R}^{N\times N}$, ensuring that oscillatory interactions evolve in a data-driven manner: $P = \frac{1}{2}(A + A^\intercal) \odot S$, where A is a trainable affinity matrix. The symmetric formulation enforces bidirectional coupling influence while maintaining neurobiological realism. The synchronization term in Eq. 1 can be redefined as $\boldsymbol{z}_i = \boldsymbol{s}_i + \sum_{j=1}^{N} p_{ij}\boldsymbol{f}_i$.

Note that a projection operation is applied to oscillatory updates onto a synchronization manifold, which prevents mode collapse and preserves diverse phase interactions:$\phi_{\boldsymbol{z}_i} = \boldsymbol{z}_i - \langle \boldsymbol{z}_i, \boldsymbol{f}_i \rangle \boldsymbol{f}_i$.

In this context, the evolution equation is reformulated as:

$$\frac{d\boldsymbol{f}_i}{dt} = \boldsymbol{\omega}_i + \lambda\phi(\boldsymbol{s}_i + \sum{}_{j=1}^{N} p_{ij}\boldsymbol{f}_i), \tag{3}$$

This projection effectively removes redundant phase components, maintaining oscillatory diversity and preventing over-constrained functional states. By iteratively refining synchronization trajectories, our method ensures that functional connectivity states emerge from structural constraints while preserving the flexibility necessary to accommodate individual variations in brain dynamics.

Hierarchical memory-driven phase stabilization via Kuramoto solver. The *Kuramoto solver* integrates hierarchical memory mechanisms to refine phase synchronization trajectories over multiple iterations. Unlike traditional SC-FC coupling models that rely on direct functional simulations, our solver iteratively adjusts synchronization states via the update rule: $\frac{d\boldsymbol{f}_i}{dt} = \Omega_i \boldsymbol{f}_i + \lambda\phi_{\boldsymbol{z}_i}$. To ensure numerical stability, all phase updates are renormalized via spherical projection: $\zeta(\boldsymbol{f}_i) = \frac{\boldsymbol{f}_i}{\|\boldsymbol{f}_i\|}$. This prevents numerical divergence, ensuring that phase evolution remains well-conditioned across solver iterations. A critical advancement in our framework is the hierarchical memory-driven refinement, where past oscillatory states are recursively integrated into the phase update mechanism:

$$F^l(t+1) = \zeta(F^l(t) + \beta\frac{dF^l(t)}{dt}), \tag{4}$$

where β is the discretization step size, our method can dynamically re-weight structural connections based on past functional interactions. This recursive learning mechanism enables long-range functional stabilization, allowing the model to iteratively adjust for transient fluctuations while preserving global oscillatory coherence. At the end of each layer l^{th}, we apply a readout function ψ_ξ^{-1} to obtain the feature representation. Ultimately, the feature representation at the final L^{th} layer is given by $\hat{F} = \psi_\xi^{-1}(F^L)$, where L denotes the number of network layers. To optimize synchronization learning, we employ a cross-entropy loss associated with the underlying clinical outcome (such as healthy or diseased), ensuring that the model effectively captures disease-related patterns in SC-FC coupling.

3.3 II: Novel Putative Synchronization-based SC–FC Coupling Biomarkers

Conceptual basis. Healthy brains operate in a *metastable* regime, flexibly transitioning between synchronized and desynchronized states to support cognition. Neurodegeneration disrupts this balance in network- and frequency-specific ways, manifesting as both *hypo*- and *hyper*-synchrony (Grieder et al., 2018; Brier et al., 2014; Hammond et al., 2007b; Shine et al., 2019). To quantify these alterations in network dynamics, we first extract a three-level hierarchy of Kuramoto Order Parameters (KOPs), then introduce a time-integrated *synchrony energy* statistic that summarizes global synchronization over time (serves as an index of *persistent phase-locking*).

Step 1 — Instantaneous phase extraction. For each node i and time point t, we reconstruct an analytic signal from the learned feature representation $F_i^l(t)$ and take its phase $\hat{\theta}_i^l(t) = \arg\{F_i^l(t) + \sqrt{-1}\,\mathcal{H}[F_i^l(t)]\}$, band-limiting to $0.01-0.1$ Hz to match infra-slow BOLD oscillations (Glerean et al., 2012; Cabral et al., 2017a; Glomb et al., 2017).

Step 2 — Region-wise KOP. The basic unit of synchrony is the region-specific order parameter $R_i^l(t) = \left|\frac{1}{M}\sum_{m=1}^{M} e^{\sqrt{-1}\hat{\theta}_{i,m}^l(t)}\right|$, where $i = 1, ..., N$ denotes the index of brain region, $m = 1, ..., M$ denotes the subjects. Because the modulus of a single oscillator is always 1, $R_i^l(t)$ acts as a *phase carrier* for downstream aggregation.

Step 3 — Subnetwork-wise KOP. Grouping regions into C subnetworks $\mathcal{C}_j$ yields $R_j^l(t) = \left|\frac{1}{N_j}\sum_{i\in\mathcal{C}_j} e^{\sqrt{-1}\hat{\theta}_i^l(t)}\right|, \quad j = 1, \ldots, C$, which captures intra-subnetwork coherence and is sensitive to subnetwork-specific dysfunction.

Step 4 — Whole-brain KOP. A global summary is obtained by averaging the regional magnitudes, $R^l_{\text{whole}}(t) = \frac{1}{N}\sum_{i=1}^{N} R^l_i(t) = \frac{1}{N}\sum_{i=1}^{N}\left|e^{\sqrt{-1}\hat{\theta}^l_i(t)}\right|$, providing a coarse but intuitive read-out of brain-wide phase coordination.

Step 4 — Synchrony Energy (time-invariant biomarker). To measure the *capacity* of each module to sustain synchrony over an entire training phase, we integrate squared coherence for subnetwork-based energy: $\mathrm{SynE}_j = \frac{1}{TL}\sum_{l=0}^{L-1}\sum_{t=0}^{T-1}\left(R^l_j(t)\right)^2$, and whole brain-based energy:

$$\mathrm{SynE}_{\text{whole}} = \frac{1}{TL}\sum\nolimits_{l=0}^{L-1}\sum\nolimits_{t=0}^{T-1}\left(R^l_{\text{whole}}(t)\right)^2. \tag{5}$$

The ℓ_2-norm in Eq. 5 encourages prolonged, high-coherence episodes while down-weighting brief coincidences. The C-dimensional vector $\mathbf{SynE} = [\mathrm{SynE}_1, \ldots, \mathrm{SynE}_C]$ and its global counterpart $\mathrm{SynE}_{\text{whole}}$ together form an interpretable, disease-sensitive SC–FC coupling signature.

Neuroscientific interpretation. SynE_j quantifies how effectively the *structural* architecture of subnetwork j facilitates ongoing *functional* synchrony. Disease-related deviations in SynE may occur in either direction: low values indicate disrupted or fragmented coupling, while abnormally high values may reflect a breakdown of adaptive desynchronization, shifting the system toward overly regular or stereotyped activity patterns. This non-monotonic relationship aligns with prior theories of disrupted metastability in neurodegeneration (Deco et al., 2017; Hellyer et al., 2014). By spanning regional, subnetwork-wise, and whole-brain scales, the putative biomarker links micro-level phase dynamics to macro-level connectome constraints, offering a principled readout for tracking disease progression.

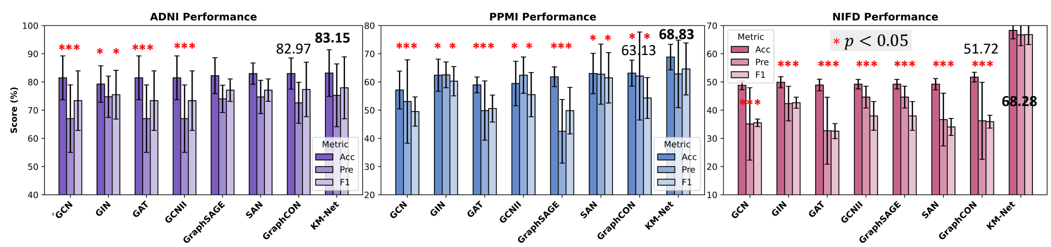

Figure 3: Performance metrics (%) on ADNI, PPMI and NIFD datasets. '*' denotes the significant improvement ($p < 0.05$).

4 Experiments

4.1 Dataset and Experimental Setup

In our experiments, we evaluate the proposed method on three publicly available neurodegenerative disease datasets. (1) Alzheimer's Disease Neuroimaging Initiative (ADNI): This dataset includes resting-state fMRI data from 135 subjects, comprising individuals diagnosed with AD and cognitively normal (CN) controls. It is designed to track brain changes associated with AD progression. (2) Parkinson's Progression Markers Initiative (PPMI): A multi-center study that collects neuroimaging data from 175 subjects, including individuals with PD, scans without evidence of dopaminergic deficit (SWEDD), prodromal PD, and CN. (3) Neuroimaging Initiative for Frontotemporal Lobar Degeneration (NIFD): This dataset focuses on FTD and includes resting-state fMRI data from 1,010 subjects. Participants are categorized into CN, logopenic variant of primary progressive aphasia (LVPPA), behavioral variant frontotemporal dementia (BV), progressive non-fluent aphasia (PNFA), and semantic variant (SV) groups. All involved data can be found and downloaded in the Image and Data Archive (IDA) [1]. The detailed demographic statistics are listed in Table 1. We utilize standardized preprocessing pipelines [2] to produce the SC and FC. In all subsequent experiments, we parcellate the brain into 116 regions using the AAL (Tzourio-Mazoyer et al., 2002) atlas, resulting

[1] https://adni.loni.usc.edu/, https://memory.ucsf.edu/research-trials/research/allftd, https://www.ppmi-info.org/.

[2] fmriprep.org/en/stable/, qsiprep.readthedocs.io/en/latest/.

Table 1: demographic characteristics of ADNI, PPMI, and NIFD cohorts.

Dataset	Size	Age		Sex		Disease stage	
		range	Mean±std	Male	Female	CN	ND
ADNI	135	55∼85	70.8±6.5	65 (48.2%)	70 (51.8%)	110 (81.5%)	25 (18.5%)
PPMI	175	40∼81	65.7±7.9	67 (38.2%)	108 (61.8%)	87 (49.7%)	88 (50.3%)
NIFD	1010	39∼88	64.8±7.7	523 (51.8%)	487 (48.2%)	490 (48.5%)	520 (51.5%)

in 116×116 SC and FC matrices (Fig. 1, middle). We further divide the whole brain into six subnetworks, including frontoparietal network (*FPN.*) visual network (*Vis.*), default mode network (*D.M.*), Ventral attention network (*V.A.*), sensorimotor network (*SM.*) and Cerebellum (*Cereb.*). Notably, while the present study adopts the widely used AAL116 parcellation, it is well recognized that atlas choice can influence SC–FC analyses (Messé, 2020; Albers et al., 2021). Systematic cross-atlas validation remains relatively rare in the connectomics literature, despite repeated calls for such evaluation (Bryce et al., 2021; Turnbull et al., 2025). We therefore acknowledge atlas dependence as a potential limitation, and suggest future work to test robustness across multiple atlases.

We implemented all models on NVIDIA H100 NVL (94GB, a total of 8 GPUs). We used a batch size of 32, a learning rate of 1×10^{-3}, and a cosine annealing schedule without warm-up. All experiments were conducted for 300 epochs. We set $L = 2$, 256 hidden channels, 25 iteration steps ($T = 25$). The Kuramoto layer used attention-based connectivity ($A =$ `"attn"`) with projection enabled. The model was initialized with $\omega = 0.01$, and the frequency length was learnable. Max-pooling was applied by default.

We compare our *KM-Net* against several graph-based approaches, including the vanilla graph neural network (GCN) (Kipf & Welling, 2016), graph isomorphism networks (GIN) (Xu et al., 2018), graph attention networks (GAT) (Veličković et al., 2017), recent popular method GCNII (Chen et al., 2020), GraphSAGE (Hamilton et al., 2017), the graph transformer with spectral attention network (SAN) (Kreuzer et al., 2021) and a graph-coupled oscillator networks (GraphCON) (Rusch et al., 2022). The graph embeddings of these methods are vectorized FCs and the adjacency matrices are SCs. For the disease diagnosis task, the ADNI dataset is formulated as a binary classification problem (AD vs. CN), the PPMI dataset as a four-class classification problem (PD, SWEDD, Prodromal, and CN), and the NIFD dataset as a five-class classification problem (CN, LVPPA, BV, PNFA, and SV). We evaluate model performance using accuracy (Acc), precision (Pre), and F1-score (F1), reporting results based on 5-fold cross-validation. The code will be released at `https://anonymous.4open.science/r/KuramNet-4EB8` upon publication.

4.2 Diagnostic Performance Across Neurodegenerative Disorders

Fig. 3 shows that *KM-Net* outperforms every competing graph model on all three cohorts in all three metrics with differences that are statistically significant (* $p < 0.05$, paired t-test). These consistencies confirm that modeling the oscillatory coupling between SC and FC reveals clinically meaningful patterns overlooked by models using only static SC or FC. The robustness of the improvements—modest but significant in ADNI, larger in PPMI, and most pronounced in NIFD—suggests that our synchronization-based framework is particularly effective when network disruptions are subtle or heterogeneous, laying the groundwork for the mechanistic, hypothesis-driven analyses that follow. We report the running time for each mode on ADNI dataset. Most standard GNNs run in 0.6–0.9 ms: GraphSAGE 0.57 (fastest), GIN 0.58, GCN 0.66, GAT 0.86, GCNII 0.82, GraphCON 0.85, with SAN at 1.02. Our *KM-Net* is also 1.02 ms, matching SAN—about 1.8× slower than GraphSAGE but still millisecond-level.

4.3 Novel Interpretation of Neurodegeneration via Neural Synchronization Biomarker

Global synchrony establishes a whole-brain baseline. We *hypothesize* that reduced neural synchronization is a putative indicator of neurodegeneration in aging brains. To test this, we quantify phase synchronization between regions using the KOP computed from the final feature representation F^L (see Methods). Fig. 4 (left) summarizes whole-brain KOP across diagnostic groups, age groups, and gender for the three cohorts. In every dataset, disease groups show a modest but systematic downward shift in mean KOP relative to CN group (ADNI: $\sim$5%; PPMI: $\sim$10%; NIFD: $< 5\%$). Because the grand-average KOP aggregates phase information over the entire cortex, even

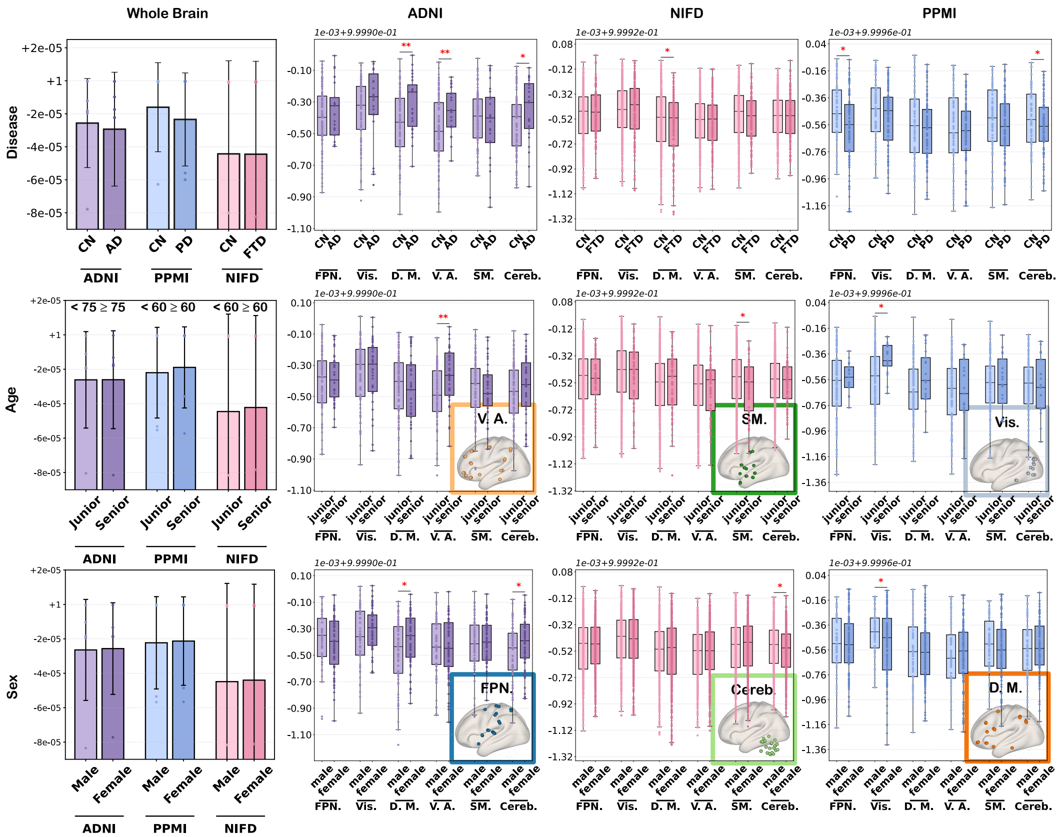

Figure 4: Whole-brain (left) and subnetwork-wise (right) Kuramoto synchrony for ADNI, PPMI and NIFD. Disease groups show lower global KOP than CN, while subnetwork-wise synchrony energy pinpoints the most affected networks—*D.M.* and *Vis.* in AD, *D.M.* in FTD, and *FPN.*, *Cereb.* in PD. Asterisks mark significant group differences (*, $p < 0.05$ **, $p < 0.001$).

subtle regional desynchronization yields small absolute changes; nevertheless, the consistent direction across AD, PD, and FTD supports the view that large-scale synchrony diminishes with neurodegeneration. By contrast, neither age (Junior vs. Senior) nor gender (Male vs. Female) produces discernible differences, indicating that the observed desynchronization is not trivially driven by demographics. Although the global effects are modest—reflecting disease heterogeneity and the dilution from whole-brain averaging—they provide a conservative benchmark. We therefore turn to a finer-grained analysis of *subnetwork-resolved* KOP to capture region-specific dysfunction, and a time–layer–integrated *synchrony-energy* measure, SynE_{whole} (Eq. 5), which indexes *persistent* phase-locking.

Subnetwork-wise synchrony reveals disorder-specific network liabilities. Moving from a whole-brain average to *subnetwork-resolved* KOPs amplifies group differences and aligns them with canonical network signatures (Fig. 4 right; asterisks denote $p < 0.05$). *(1) ADNI* — Within-network KOP is elevated in patients relative to CN in the *default-mode network (D.M.)* and, to a lesser extent, the *visual network (Vis.)* (Buckner et al., 2005). Higher KOP indicates stronger *instantaneous* synchrony, consistent with a loss of adaptive desynchronization under E–I imbalance (Palop & Mucke, 2016). Thus, the subnetwork-wise KOP captures a transmodal (*D.M.*) plus posterior-sensory pattern of hypersynchrony in early AD. *(2) NIFD* — The *D.M.* is the only subnetwork exhibiting a significant decline, indicating reduced intra-network synchrony; this mirrors anterior cingulo-frontal decoupling in behavioural-variant FTD (Seeley et al., 2009) and accords with its social-cognitive and executive impairments. *(3) PPMI* — PD shows lower within-network KOP than CN in the *frontoparietal network (FPN.)* and *cerebellum*, indicating reduced intra-network synchrony. This fits with dopamine depletion disrupting basal ganglia–thalamo–cortical and cerebello–thalamo–cortical loops, weakening executive circuitry and timing/sensorimotor integration; although compensatory increases are sometimes reported, early drug-naïve PD typically exhibits diminished network coherence (Boon et al., 2020; Luo et al., 2014; Lefaivre et al., 2016). Age- and gender-related

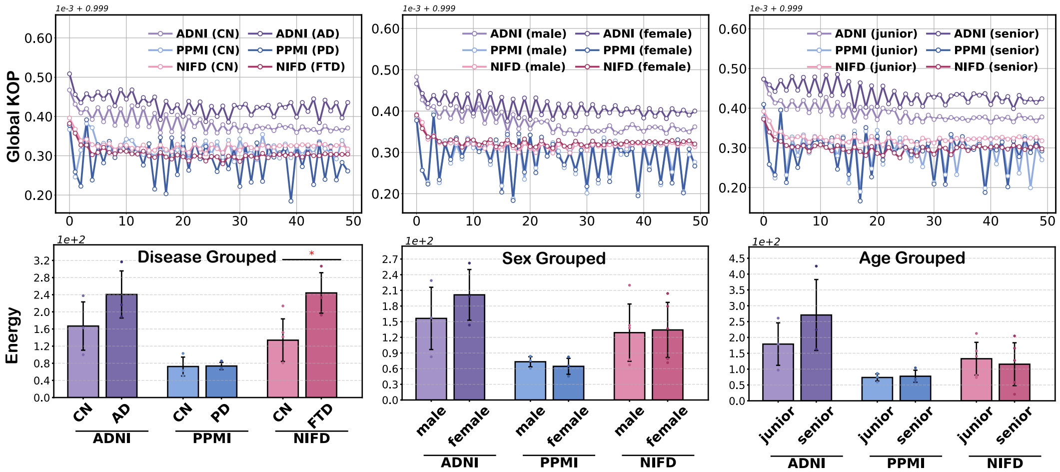

Figure 5: Global (whole brain) Kuramoto synchrony across 50 iterations (top) and its time–layer-integrated energy (bottom). Disease groups show lower and more volatile KOP than controls, especially in PD, while age and gender have negligible impact. Synch-energy is elevated in AD and FTD, indicating more persistent phase-locking; PD shows only a modest increase.

effects are modest and subnetwork-specific—significant contrasts appear occasionally (e.g., age: ADNI–*FPN.*, NIFD–*D.M.*, PPMI–*Vis.*; gender: ADNI–*Vis.*, NIFD–*SM.*, PPMI–*Cerebellum*) and are clearly smaller than the disease-group effects.

Iteration- and layer-resolved analysis of global synchrony. Fig. 5 tracks the *global* KOP (whole brain, Eq. 5) across 50 numerical integration steps (top) and encodes the same information into a single synchrony-energy scalar (bottom; Eq. 5). Two features stand out: *(1) Slower convergence and lower plateaus in disease.* Disease trajectories equilibrate more slowly and $\sim$10–20% lower than CN, implying a weaker-synchrony attractor and aligning with models where reduced structural coupling delays global phase alignment (Cabral et al., 2017b). *(2) Pronounced temporal volatility in Parkinson's disease.* PPMI trajectories show larger peak-to-trough excursions—consistent with burst-like β oscillations in PD—indicating rapid alternations between synchronized and desynchronized states (Hammond et al., 2007a; Herz et al., 2017). *Energy read-out.* SynE is elevated in AD (ADNI) and highest in FTD (NIFD; $p < 0.05$), indicating more *persistent* phase-locking (hypersynchrony) and reduced adaptive desynchronization in these dementias (Palop & Mucke, 2016; Zhou & Seeley, 2014). In contrast, PD (PPMI) shows only a modest, non-significant change relative to CN, consistent with transient, burst-driven dynamics rather than a sustained shift in global synchrony (Hammond et al., 2007a; Herz et al., 2017). *Minimal demographic influence.* Compared with the clinical groups, age- and gender-related differences are minor in both the temporal and energy domains, reinforcing that the observed synchrony changes are driven primarily by disease rather than by demographic factors.

Taken together, a lower global mean KOP accompanied by a higher whole-brain SynE suggests that neurodegeneration yields fewer but longer-lasting bouts of synchrony: overall average coupling is weakened, yet the episodes that do emerge remain phase-locked for longer, reflecting more persistent hypersynchrony when it occurs.

5 Conclusion

In this work, we presented *KM-Net*, a brain-inspired deep Kuramoto framework that links structural connectomes to phase-synchrony dynamics. By modelling how oscillatory synchrony emerges from structural coupling, *KM-Net* yields an interpretable, biologically grounded representation of whole-brain fluctuations. Across three independent cohorts, our *KM-Net* achieved state-of-the-art diagnostic accuracy for AD, PD and FTD and exposed disorder-specific vulnerabilities. At the macroscale, disease groups showed a distinctive burst-like synchrony regime: global mean KOP was lower, yet whole-brain SynE was higher, indicating fewer but longer-lasting episodes of hypersynchrony. Taken together, our results demonstrate the potential of neural-synchrony modelling to advance computational neuroscience and provide a practical, interpretable tool for early detection and longitudinal tracking of neurodegenerative progression.

REFERENCES

Farras Abdelnour, Henning U Voss, and Ashish Raj. Network diffusion accurately models the relationship between structural and functional brain connectivity networks. *Neuroimage*, 90:335–347, 2014.

Kristoffer J Albers, Karen S Ambrosen, Matthew G Liptrot, Tim B Dyrby, Mikkel N Schmidt, and Morten Mørup. Using connectomics for predictive assessment of brain parcellations. *NeuroImage*, 238:118170, 2021.

Bastiaan R Bloem, Michael S Okun, and Christine Klein. Parkinson's disease. *The Lancet*, 397 (10291):2284–2303, 2021.

Lennard I Boon, Dagmar H Hepp, Linda Douw, Noëlle van Geenen, Tommy AA Broeders, Jeroen JG Geurts, Henk W Berendse, and Menno M Schoonheim. Functional connectivity between resting-state networks reflects decline in executive function in parkinson's disease: A longitudinal fmri study. *NeuroImage: Clinical*, 28:102468, 2020.

Matthew R Brier, Jewell B Thomas, Anne M Fagan, Jason Hassenstab, David M Holtzman, Tammie L Benzinger, John C Morris, and Beau M Ances. Functional connectivity and graph theory in preclinical alzheimer's disease. *Neurobiology of aging*, 35(4):757–768, 2014.

Nessa V Bryce, John C Flournoy, João F Guassi Moreira, Maya L Rosen, Kelly A Sambook, Patrick Mair, and Katie A McLaughlin. Brain parcellation selection: An overlooked decision point with meaningful effects on individual differences in resting-state functional connectivity. *NeuroImage*, 243:118487, 2021.

Randy L Buckner, Abraham Z Snyder, Benjamin J Shannon, Gina LaRossa, Rimmon Sachs, Anthony F Fotenos, Yvette I Sheline, William E Klunk, Chester A Mathis, John C Morris, et al. Molecular, structural, and functional characterization of alzheimer's disease: evidence for a relationship between default activity, amyloid, and memory. *Journal of neuroscience*, 25(34):7709–7717, 2005.

Joana Cabral, Etienne Hugues, Olaf Sporns, and Gustavo Deco. Role of local network oscillations in resting-state functional connectivity. *Neuroimage*, 57(1):130–139, 2011.

Joana Cabral, Morten L Kringelbach, and Gustavo Deco. Functional connectivity dynamically evolves on multiple time-scales over a static structural connectome: Models and mechanisms. *NeuroImage*, 160:84–96, 2017a.

Joana Cabral, Diego Vidaurre, Paulo Marques, Ricardo Magalhães, Pedro Silva Moreira, José Miguel Soares, Gustavo Deco, Nuno Sousa, and Morten L Kringelbach. Cognitive performance in healthy older adults relates to spontaneous switching between states of functional connectivity during rest. *Scientific reports*, 7(1):5135, 2017b.

Ming Chen, Zhewei Wei, Zengfeng Huang, Bolin Ding, and Yaliang Li. Simple and deep graph convolutional networks. In *International Conference on Machine Learning*, pp. 1725–1735. PMLR, 2020.

Jeffrey Cummings. Disease modification and neuroprotection in neurodegenerative disorders. *Translational Neurodegeneration*, 6:1–7, 2017.

Tingting Dan, Minjeong Kim, Won Hwa Kim, and Guorong Wu. Uncovering structural-functional coupling alterations for neurodegenerative diseases. In *International Conference on Medical Image Computing and Computer-Assisted Intervention*, pp. 87–96. Springer, 2023.

Gustavo Deco, Morten L Kringelbach, Viktor K Jirsa, and Petra Ritter. The dynamics of resting fluctuations in the brain: metastability and its dynamical cortical core. *Scientific reports*, 7(1): 3095, 2017.

Michael C Donohue, Reisa A Sperling, Ronald Petersen, Chung-Kai Sun, Michael W Weiner, Paul S Aisen, Alzheimer's Disease Neuroimaging Initiative, et al. Association between elevated brain amyloid and subsequent cognitive decline among cognitively normal persons. *Jama*, 317(22): 2305–2316, 2017.

Alexander J Ehrenberg, Ayesha Khatun, Emma Coomans, Matthew J Betts, Federica Capraro, Elisabeth H Thijssen, Konstantin Senkevich, Tehmina Bharucha, Mehrsa Jafarpour, Peter NE Young, et al. Relevance of biomarkers across different neurodegenerative diseases. *Alzheimer's research & therapy*, 12:1–11, 2020.

Enrico Glerean, Juha Salmi, Juha M Lahnakoski, Iiro P Jääskeläinen, and Mikko Sams. Functional magnetic resonance imaging phase synchronization as a measure of dynamic functional connectivity. *Brain connectivity*, 2(2):91–101, 2012.

Katharina Glomb, Adrián Ponce-Alvarez, Matthieu Gilson, Petra Ritter, and Gustavo Deco. Resting state networks in empirical and simulated dynamic functional connectivity. *NeuroImage*, 159: 388–402, 2017.

Joaquín Goñi, Martijn P Van Den Heuvel, Andrea Avena-Koenigsberger, Nieves Velez de Mendizabal, Richard F Betzel, Alessandra Griffa, Patric Hagmann, Bernat Corominas-Murtra, Jean-Philippe Thiran, and Olaf Sporns. Resting-brain functional connectivity predicted by analytic measures of network communication. *Proceedings of the National Academy of Sciences*, 111(2): 833–838, 2014.

Matthias Grieder, Danny JJ Wang, Thomas Dierks, Lars-Olof Wahlund, and Kay Jann. Default mode network complexity and cognitive decline in mild alzheimer's disease. *Frontiers in neuroscience*, 12:770, 2018.

Will Hamilton, Zhitao Ying, and Jure Leskovec. Inductive representation learning on large graphs. *Advances in neural information processing systems*, 30, 2017.

Christian Hammond, Hagai Bergman, and Peter Brown. Pathological synchronization in Parkinson's disease: Networks, models and treatments, 2007a.

Constance Hammond, Hagai Bergman, and Peter Brown. Pathological synchronization in parkinson's disease: networks, models and treatments. *Trends in neurosciences*, 30(7):357–364, 2007b.

Michał Harciarek and Stephanie Cosentino. Language, executive function and social cognition in the diagnosis of frontotemporal dementia syndromes. *International Review of Psychiatry*, 25(2): 178–196, 2013.

Peter J Hellyer, Murray Shanahan, Gregory Scott, Richard JS Wise, David J Sharp, and Robert Leech. The control of global brain dynamics: opposing actions of frontoparietal control and default mode networks on attention. *Journal of Neuroscience*, 34(2):451–461, 2014.

Damian M. Herz, Simon Little, David J. Pedrosa, Maarten Speekenbrink, Anja Horn, Rafal Bogacz, and Peter Brown. Mechanisms underlying decision-making in the mothers of Parkinson's disease: The role of oscillatory bursts. *Proceedings of the National Academy of Sciences*, 114(49): E10494–E10503, 2017. doi: 10.1073/pnas.1702512114.

Christopher J Honey, Olaf Sporns, Leila Cammoun, Xavier Gigandet, Jean-Philippe Thiran, Reto Meuli, and Patric Hagmann. Predicting human resting-state functional connectivity from structural connectivity. *Proceedings of the National Academy of Sciences*, 106(6):2035–2040, 2009.

Willemijn J Jansen, Rik Ossenkoppele, Dirk L Knol, Betty M Tijms, Philip Scheltens, Frans RJ Verhey, Pieter Jelle Visser, Pauline Aalten, Dag Aarsland, Daniel Alcolea, et al. Prevalence of cerebral amyloid pathology in persons without dementia: a meta-analysis. *Jama*, 313(19):1924–1938, 2015.

Andreas Jeromin and Robert Bowser. Biomarkers in neurodegenerative diseases. *Neurodegenerative diseases: pathology, mechanisms, and potential therapeutic targets*, pp. 491–528, 2017.

Thomas N Kipf and Max Welling. Semi-supervised classification with graph convolutional networks. *arXiv preprint arXiv:1609.02907*, 2016.

Devin Kreuzer, Dominique Beaini, Will Hamilton, Vincent Létourneau, and Prudencio Tossou. Rethinking graph transformers with spectral attention. *Advances in Neural Information Processing Systems*, 34:21618–21629, 2021.

Yoshiki Kuramoto. Self-entrainment of a population of coupled non-linear oscillators. In *International symposium on mathematical problems in theoretical physics: January 23–29, 1975, kyoto university, kyoto/Japan*, pp. 420–422. Springer, 1975.

Anthony E Lang. Clinical trials of disease-modifying therapies for neurodegenerative diseases: the challenges and the future. *Nature medicine*, 16(11):1223–1226, 2010.

Shannon C Lefaivre, Matt JN Brown, and Quincy J Almeida. Cerebellar involvement in parkinson's disease resting tremor. *Cerebellum & Ataxias*, 3(1):13, 2016.

Bai Li, Xue Chen, Yue Yuan, and Yanjiang Wang. Analyzing the relationship between human brain structural and functional connectivity using kuramoto model. In *2018 14th IEEE International Conference on Signal Processing (ICSP)*, pp. 774–779. IEEE, 2018.

ChunYan Luo, Wei Song, Qin Chen, ZhenZhen Zheng, Ke Chen, Bei Cao, Jing Yang, JianPeng Li, XiaoQi Huang, QiYong Gong, et al. Reduced functional connectivity in early-stage drug-naive parkinson's disease: a resting-state fmri study. *Neurobiology of aging*, 35(2):431–441, 2014.

Badhan Mazumder, Ayush Kanyal, Lei Wu, Vince D. Calhoun, and Dong Hye Ye. Physics-guided multi-view graph neural network for schizophrenia classification via structural-functional coupling. In *International Workshop on PRedictive Intelligence In MEdicine*, pp. 61–73. Springer, 2024.

Arnaud Messé. Parcellation influence on the connectivity-based structure–function relationship in the human brain. *Human brain mapping*, 41(5):1167–1180, 2020.

Vladislav Myrov, Alina Suleimanova, Samanta Knapič, Paula Partanen, Maria Vesterinen, Wenya Liu, Satu Palva, and J Matias Palva. Hierarchical whole-brain modeling of critical synchronization dynamics in human brains. *bioRxiv*, pp. 2024–05, 2024.

Jorge J Palop and Lennart Mucke. Network abnormalities and interneuron dysfunction in alzheimer disease. *Nature Reviews Neuroscience*, 17(12):777–792, 2016.

Johanna L Popp, Jonas A Thiele, Joshua Faskowitz, Caio Seguin, Olaf Sporns, and Kirsten Hilger. Structural-functional brain network coupling during cognitive demand reveals intelligence-relevant communication strategies. *Communications Biology*, 8(1):855, 2025.

Martin Prince, Anders Wimo, Maëlenn Guerchet, Gemma-Claire Ali, Yu-Tzu Wu, and Matthew Prina. *World Alzheimer Report 2015. The Global Impact of Dementia: An analysis of prevalence, incidence, cost and trends.* PhD thesis, Alzheimer's Disease International, 2015.

Adam C Rayfield, Taotao Wu, Jared A Rifkin, and David F Meaney. Individualized mouse brain network models produce asymmetric patterns of functional connectivity after simulated traumatic injury. *Network Neuroscience*, 9(1):326–351, 2025.

Francisco A Rodrigues, Thomas K DM Peron, Peng Ji, and Jürgen Kurths. The kuramoto model in complex networks. *Physics Reports*, 610:1–98, 2016.

T Konstantin Rusch, Ben Chamberlain, James Rowbottom, Siddhartha Mishra, and Michael Bronstein. Graph-coupled oscillator networks. In *International Conference on Machine Learning*, pp. 18888–18909. PMLR, 2022.

Philip Scheltens, Bart De Strooper, Miia Kivipelto, Henne Holstege, Gael Chételat, Charlotte E Teunissen, Jeffrey Cummings, and Wiesje M van der Flier. Alzheimer's disease. *The Lancet*, 397 (10284):1577–1590, 2021.

William W Seeley, Richard K Crawford, Juan Zhou, Bruce L Miller, and Michael D Greicius. Neurodegenerative diseases target large-scale human brain networks. *Neuron*, 62(1):42–52, 2009.

James M Shine, Michael Breakspear, Peter T Bell, Kaylena A Ehgoetz Martens, Richard Shine, Oluwasanmi Koyejo, Olaf Sporns, and Russell A Poldrack. Human cognition involves the dynamic integration of neural activity and neuromodulatory systems. *Nature neuroscience*, 22(2): 289–296, 2019.

Yibao Sun, Pan Wang, Kun Zhao, Pindong Chen, Yida Qu, Zhuangzhuang Li, Suyu Zhong, Bo Zhou, Jie Lu, Xi Zhang, et al. Structure–function coupling reveals the brain hierarchical structure dysfunction in alzheimer's disease: A multicenter study. *Alzheimer's & Dementia*, 20 (9):6305–6315, 2024.

Adam Turnbull, Feng Vankee Lin, and Zhengwu Zhang. Issues of parcellation in the calculation of structure–function coupling. *Nature Reviews Neuroscience*, 26(1):60–60, 2025.

Nathalie Tzourio-Mazoyer, Brigitte Landeau, Dimitri Papathanassiou, Fabrice Crivello, Octave Etard, Nicolas Delcroix, Bernard Mazoyer, and Marc Joliot. Automated anatomical labeling of activations in spm using a macroscopic anatomical parcellation of the mni mri single-subject brain. *Neuroimage*, 15(1):273–289, 2002.

Petar Veličković, Guillem Cucurull, Arantxa Casanova, Adriana Romero, Pietro Lio, and Yoshua Bengio. Graph attention networks. *arXiv preprint arXiv:1710.10903*, 2017.

David A Wolk, Carl Sadowsky, Beth Safirstein, Juha O Rinne, Ranjan Duara, Richard Perry, Marc Agronin, Jose Gamez, Jiong Shi, Adrian Ivanoiu, et al. Use of flutemetamol f 18–labeled positron emission tomography and other biomarkers to assess risk of clinical progression in patients with amnestic mild cognitive impairment. *JAMA neurology*, 75(9):1114–1123, 2018.

Han Wu, Yinping Lu, Luyao Wang, Jinglong Wu, Ying Liu, and Zhilin Zhang. Dynamic and static structure–function coupling with machine learning for the early detection of alzheimer's disease. *Human Brain Mapping*, 46(5):e70202, 2025.

Keyulu Xu, Weihua Hu, Jure Leskovec, and Stefanie Jegelka. How powerful are graph neural networks? *arXiv preprint arXiv:1810.00826*, 2018.

Ruwei Yao, Yichao Li, Xintong Yao, Kang Wang, Jingling Qu, Xiaolong Zou, and Bo Hong. Brain wave dynamics in a hopfield-kuramoto model. *Physical Review E*, 111(4):044310, 2025.

Juan Zhou and William W Seeley. Network dysfunction in alzheimer's disease and frontotemporal dementia: implications for psychiatry. *Biological psychiatry*, 75(7):565–573, 2014.

Ting Zou, Chen Chen, Huafu Chen, Xuyang Wang, Lin Gan, Chong Wang, Qing Gao, Chunyan Zhang, Wei Liao, Jingliang Cheng, et al. Structural-functional connectivity decoupling in multi-scale brain networks in parkinson's disease. *BMC neuroscience*, 25(1):78, 2024.